The American Journal of Pathology, Vol. 184, No. 7, July 2014

ELSEVIER

The American Journal of
PATHOLOGY
ajp.amjpathol.org

IMMUNOPATHOLOGY AND INFECTIOUS DISEASES

Characterization of a Novel Necrotic Granuloma Model of Latent Tuberculosis Infection and Reactivation in Mice

Noton K. Dutta,* Peter B. Illei,† Sanjay K. Jain,* and Petros C. Karakousis*‡

From the Departments of Medicine and Pathology,† Johns Hopkins University School of Medicine, Baltimore; and the Department of International Health,‡ Johns Hopkins Bloomberg School of Public Health, Baltimore, Maryland*

Accepted for publication March 18, 2014.

Address correspondence to Petros C. Karakousis, M.D., Center for Tuberculosis Research, Johns Hopkins University School of Medicine, 1550 Orleans St, Room 110, Baltimore, MD 21287. E-mail: petros@jhmi.edu.

We sought to develop and characterize a novel paucibacillary model in mice, which develops necrotic lung granulomas after infection with *Mycobacterium tuberculosis*. Six weeks after aerosol immunization with recombinant *Mycobacterium bovis* bacillus Calmette-Guerin overexpressing the 30-kDa antigen, C3HeB/FeJ mice were aerosol infected with *M. tuberculosis* H37Rv. Six weeks later, mice were treated with one of three standard regimens for latent tuberculosis infection or tumor necrosis factor (TNF)—neutralizing antibody. Mouse lungs were analyzed by histological features, positron emission tomography/computed tomography, whole-genome microarrays, and RT-PCR. Lungs and sera were studied by multiplex enzyme-linked immunosorbent assays. Paucibacillary infection was established, recapitulating the sterilizing activities of human latent tuberculosis infection regimens. TNF neutralization led to increased lung bacillary load, disrupted granuloma architecture with expanded necrotic foci and reduced tissue hypoxia, and accelerated animal mortality. TNF-neutralized mouse lungs and sera showed significant up-regulation of interferon γ, IL-1β, IL-6, IL-10, chemokine ligands 2 and 3, and matrix metalloproteinase genes. Clinical and microbiological reactivation of paucibacillary infection by TNF neutralization was associated with reduced hypoxia in lung granulomas and induction of matrix metalloproteinases and proinflammatory cytokines. This model may be useful for screening the sterilizing activity of novel anti-tuberculosis drugs, and identifying mycobacterial regulatory and metabolic pathways required for bacillary growth restriction and reactivation. *(Am J Pathol 2014, 184: 2045—2055; http://dx.doi.org/10.1016/j.ajpath.2014.03.008)*

Progress in understanding latent tuberculosis (TB) infection (LTBI) has been impeded by the difficulty in obtaining relevant host tissue and microbiological samples from persons latently infected with *Mycobacterium tuberculosis* (*Mtb*) and by the lack of adequate research models and molecular tools. Unlike human LTBI, the classic mouse model of TB infection is characterized by a high bacillary burden with progressive lung pathological features and early mouse death.[1] Depending on the initial inoculum of *Mtb*, bacillary numbers can exceed 10^6 to 10^7 in the lungs of nonimmunized mice by the onset of adaptive immunity, and the animals generally survive for 1 to 3 months after infection. Previous studies have shown that *Mycobacterium bovis* bacillus Calmette-Guerin (BCG)-immunized BALB/c mice are able to effectively limit bacillary growth after *Mtb* aerosol challenge and do not succumb to infection.[2,3] More important, the relatively small bacillary population established exhibits greater susceptibility to rifampin (R) relative to isoniazid (H), mirroring anti-tubercular susceptibility profiles observed in LTBI.[4] However, a major deficiency is that the lung lesions lack caseation necrosis, which is the pathological hallmark of human TB granulomas,[5,6] in which bacilli are believed to reside during LTBI.[7] Larger animal models faithfully represent many features of human LTBI but are expensive and not widely available.[8,9] The ideal model would combine the availability, economy, and superior tractability of mice with key features of LTBI, including the establishment of a paucibacillary infection within necrotic lung granulomas, as observed in larger animal models.

Supported by the National Heart, Lung, and Blood Institute and the National Institute of Allergy and Infectious Diseases of the NIH awards R01HL106786 and R01AI083125, respectively. The funding sources had no role in the study design, data collection, data analysis, data interpretation, or writing of the report. The content is solely the responsibility of the authors and does not necessarily represent the official views of the NIH.

Disclosures: None declared.

http://dx.doi.org/10.1016/j.ajpath.2014.03.008

Recently, there has been significant interest in C3HeB/FeJ mice, which lack expression of *Ipr1* and develop well-circumscribed TB lung granulomas with central necrosis[10] and tissue hypoxia,[11] as observed in larger animal models.[12] Because of these favorable features, this mouse strain has been used recently to test the efficacy of various anti-tubercular regimens and novel anti-inflammatory therapies.[13–16]

Herein, we vaccinated C3HeB/FeJ mice with a recombinant BCG strain overexpressing the 30-kDa antigen[17] to develop a novel model of paucibacillary infection. We found that this model faithfully represents the hierarchy of sterilizing activities of standard LTBI regimens.[18] By using the tumor necrosis factor (TNF)—neutralizing antibody, MP6-XT22, which has been shown to exacerbate chronic TB in mice to effect reactivation,[19] we characterized the progression from latent to active infection in live animals using positron emission tomography (PET)/computed tomography (CT) imaging, and post-mortem by microbiological, histopathological, and immunohistochemistry (IHC) using a hypoxia-specific probe. Finally, we characterized the cytokine profiles in the lungs and sera of mice before and after reactivation of infection.

Materials and Methods

Mtb Strains

A recombinant *M. bovis* BCG strain overexpressing the 30-kD major secretory protein (rBCG30)[2,3] and *Mtb* H37Rv (Johns Hopkins University, Baltimore, MD)[20] were used. rBCG30 was used as an immunizing agent because it is more immunogenic in mice than the parent BCG Tice strain and has a hygromycin resistance selection marker to differentiate it from *Mtb*.[21]

Antibiotic Therapy and TNF Neutralization

Separate groups of mice were randomized to receive daily (5 days per week) oral treatment with human-equivalent doses of H, 10 mg/kg, R, 10 mg/kg alone, or R, 10 mg/kg with pyrazinamide (Z), 150 mg/kg, which was initiated 6 weeks after infection (day 0).[11,15] Antibiotics were discontinued for groups of 15 mice after completion of 2 or 4 months of treatment for relapse assessment (Table 1).

TNF-neutralizing agent, MP6-XT22 (rat IgG1),[19,22] was purified from cell culture of a hybridoma obtained from DNAX by the National Cell Culture Center and injected (0.5 mg i.p.) twice weekly per mouse for 4 weeks.[23]

Animals

A total of 217 female C3HeB/FeJ mice (aged 5 to 6 weeks; Jackson Laboratory, Bar Harbor, ME) were used in this study. Animals were housed in a biosafety level 3, specific pathogen-free facility and fed water and chow ad libitum. All protocols were approved by the Animal Care and Use Committee, Biosafety, and Radiation Safety offices at Johns Hopkins University School of Medicine (Baltimore, MD).

Aerosol BCG Immunization and Challenge with *Mtb*

By using the inhalation exposure system (Glas-Col, Terre Haute, IN), mice were immunized with log-phase cultures (OD_{600}, approximately 0.6) of rBCG30[17] and infected 6 weeks later using a 1:2000 dilution of a 7-day-old broth culture of *Mtb* $H_{37}Rv$ (OD_{600}, approximately 1.0).

PET/CT Imaging

Live C3HeB/FeJ mice were imaged at 6 weeks after immunization, 6 weeks after infection, and 4 weeks after TNF neutralization. [^{18}F] 2-fluoro-deoxy-D-glucose ([^{18}F]FDG)-PET or copper(II)-diacetyl-bis(N^4-methylthiosemicarbazone) ([^{64}Cu]ATSM)-PET imaging was performed.[11,24] All images were reconstructed and coregistered with CT images using either Amide version 0.9.1 (*http://amide.sourceforge.net*), or Amira version 5.2.2 (Visage Imaging, San Diego, CA), and standardized uptake values computed.[11]

Table 1 Basic Experimental Scheme

Variable	No. of mice sacrificed at the given time points*							Experiments for		
Group†	W-12	W-6	W0	W4	W6	W8	W16	Imaging	Time to death analysis	Total mice
Uninfected								4		4
Infected untreated	5	5	5	5		5 (+12)	5 (+12)	4	15	49
TNF-α‡				5	5			4	15	29
H_{10}				5		5 (+15)	5 (+15)			45
R_{10}				5		5 (+15)	5 (+15)			45
$R_{10}Z_{150}$				5		5 (+15)	5 (+15)			45
Total mice	5	5	5	25	5	20	25			217

Values in the table are numbers of animals.

*Time points: week −12, immunization with rBCG30 via aerosol 12 weeks before treatment; week −6, low-dose aerosol challenge with *Mtb* 6 weeks before treatment; week 0, day of treatment initiation; week 4, 1 month after treatment initiation, and so on. (+12) signifies that the indicated number of mice were held for 12 additional weeks beyond the completion of treatment before being sacrificed to determine the proportion with culture-positive relapse.

†Drug doses (mg/kg) as indicated by subscripts. Doses of each drug were determined to be equivalent on the basis of area under the serum concentration-time curve and were given daily (5 of 7 days) by gavage.

‡Anti—TNF-α treatment, 0.5 mg i.p. twice weekly per mouse for 1 month.

W, week.

Clinical, Histopathological, and Microbiological End Points

Total body, lung, and spleen weights were recorded, and lungs and spleens were examined for visible lesions at the time of sacrifice. Lung samples were placed into 10% buffered formaldehyde, processed, and paraffin embedded for histological staining with H&E and Kinyoun stain for acid-fast bacilli (AFB) detection. Remaining lung samples were homogenized and plated in parallel on the following: i) selective Middlebrook 7H11 agar (Becton-Dickinson, Baltimore, MD) containing 10% oleic acid—albumin—dextrose—catalase, ii) 7H11 agar supplemented with 40 mg/mL of hygromycin (Roche Diagnostics, Indianapolis, IN) to select for rBCG30, and iii) 7H11 agar supplemented with 4 mg/mL of 2-thiophenecarboxylic acid hydrazide (TCH; Sigma, St. Louis, MO) to select for *Mtb* colonies.[25] Plates were incubated at 37°C for 6 weeks for colony-forming unit (CFU) determination. Relapse was defined as a positive culture result on plating entire undiluted lung homogenates.

TNF Bioassay

To ensure that MP6-XT22, a rat IgG1 monoclonal antibody, reduced local TNF activity in mouse lung tissues, functional TNF activity and levels were measured by the WEHI assay and enzyme-linked immunosorbent assay (please see *Confirmation of Transcriptional Data by Multiplex Cytokine Analysis*), respectively. TNF bioactivity was measured in filter (0.22-μm)—sterilized lung homogenates using the WEHI assay.[26] WEHI13-VAR cells (ATCC, Manassas, VA) were plated at 1.5×10^5 per well in 96-well plates (Becton Dickinson), and serial dilutions of experimental lung homogenates or standard recombinant mouse TNF (BioLegend, San Diego, CA) were added to each well and incubated for 24 hours. To each well, 100 mg of 3-(4,5-dimethylthiazol-2-yl)-2,5-diphenyltetrazolium bromide was added and incubated at 37°C for 4 hours. Dimethyl sulfoxide was added and plates were read at 595 nm. Levels of TNF in experimental samples were calculated on the basis of a standard curve for recombinant TNF.

Pimonidazole IHC

Mice were injected i.p. with 60 mg/kg pimonidazole hydrochloride at least 1.5 hours before sacrifice, and lungs and kidneys were harvested, fixed, and stained with a hypoxyprobe staining kit (Hypoxyprobe, Inc, Burlington, MA).[11,27] Uninfected C3HeB/FeJ mouse lungs and kidney sections containing hypoxic renal tubular cells served as negative and positive controls, respectively.[27]

Microarray Experiments and Pathway Analysis

Total RNA was extracted from frozen lungs using the RiboPure Kit plus DNA-free reagents (Ambion, Grand Island, NY). cRNA samples were prepared using an Illumina TotalPrep RNA Amplification Kit (Ambion) and hybridized to Illumina Mouse WG-6 version 2.0 BeadArrays (San Diego, CA) according to manufacturer's protocols. Raw and normalized array results were deposited into an National Center for Biotechnology Information Gene Expression Omnibus database (*http://www.ncbi.nlm.nih.gov/geo*; accession number GSE55183). Genes whose expression changed by at least twofold ($P < 0.05$) were considered significantly differentially expressed.[28]

Pathway analysis was performed by uploading statistically significant ($P < 0.05$) data set(s) into an Ingenuity Pathways Analysis algorithm (Ingenuity Systems, Redwood City, CA).[28]

Quantitative RT-PCR

To validate transcriptomic results, the mouse RT_2ProfilerPCR arrays for Cytokines and Chemokines (PAMM-150Z) and hypoxia signaling pathway (PAMM-032Z) (SA Biosciences, Frederick, MD) were used, using an ABI 7500 real-time PCR machine (Applied Biosystems, Grand Island, NY). The data for biological duplicates were analyzed using the SA Biosciences PCR Array Data Analysis Software (*http://www.sabiosciences.com/pcr/arrayanalysis.php*, last accessed December 2012).[28]

LCM and RT-PCR

Tissue processing and laser capture microdissection (LCM) were performed as per PALM MicroLaser systems protocols (Carl Zeiss MicroImaging, Munich, Germany). Total RNA from stained (LCM Staining Kit Reagents; Ambion), pooled granulomatous tissue of formalin-fixed, paraffin-embedded lung sections was isolated using an RNeasy Micro Kit (Qiagen, Frederick, MD), and cDNA was synthesized using a Transcriptor First Strand cDNA Synthesis Kit (Roche Diagnostics). RT-PCR was performed using Power SYBR Green PCR Master Mix (Invitrogen, Grand Island, NY) and gene-specific primers for mouse hypoxia-inducible factor 1α, vascular endothelial growth factor (VEGF), matrix metalloproteinase (MMP)-9, and glyceraldehyde-3-phosphate dehydrogenase. Gene expression data were normalized to the housekeeping gene glyceraldehyde-3-phosphate dehydrogenase.

Confirmation of Transcriptional Data by Multiplex Cytokine Analysis

Murine cytokine levels were quantified from whole lung homogenates and serum using a microbead-based Bio-plex method (Bioplex mouse cytokine group 1, 23-plex assay; Bio-Rad Laboratories, Hercules, CA) and a Bioplex-200 apparatus (Luminex, Austin, TX).[28]

Statistical Analysis

Pairwise comparisons of group mean values for organ weights and $\log_{10}$-transformed CFU counts were made using Student's

t-test, and one-way analysis of variance and Bonferroni's post test with GraphPad InStat, version 3.05 (GraphPad, San Diego, CA). Comparisons of the normalized mean PET lung activity data among experimental groups were performed by *U*-test. For each analysis, five mice were used at each time point, except for relapse groups, in which 15 mice were used.

Results

Establishment and Validation of a Novel Paucibacillary Mouse Model

Mice were immunized via aerosol with rBCG30, resulting in a means ± SD implanted lung CFU count of 3.61 ± 0.07 $\log_{10}$. Six weeks later, mean lung rBCG30 CFU counts had increased to 5.86 ± 0.18 $\log_{10}$. On the day after aerosol challenge, the mean *Mtb* lung CFU count in the lungs was 1.36 ± 0.03 $\log_{10}$. Six weeks later (day 0 of treatment), the mean *Mtb* lung bacillary count was 4.24 ± 0.13 $\log_{10}$ (Figure 1). All regimens displayed bactericidal activity, and the rank order of potency was consistent with that against human LTBI.[18] Thus, RZ was significantly more active than H or R alone by week 4 ($P < 0.0001$), and rendered all mouse lungs culture negative by week 8. All 15 mice receiving 2 months of R and H monotherapy showed relapse, whereas only 60% of RZ-treated animals relapsed ($P < 0.01$). Treatment with R and RZ for 4 months resulted in relapse rates of 30% and 0%, respectively.

No significant differences were observed between treatment groups in mean total body weights or normalized mean organ weights over time. However, gross pathological characteristics revealed a marked reduction in the number and size of lung tubercles in the RZ group within 8 weeks of treatment initiation (data not shown).

Reactivation of Infection with TNF Neutralization

Compared with untreated mice, local TNF activity in the lung homogenates of MP6-XT22–treated mice was significantly ($P < 0.01$) reduced (Figure 2A), confirming systemic neutralization of TNF by MP6-XT22. Weight loss was significantly greater in anti–TNF-treated mice relative to untreated controls ($P < 0.0001$) (Figure 2B). The median survival time of mice was 34 days after anti-TNF therapy (Figure 2C), compared with 200 days in control mice ($P < 0.0001$). Although we cannot exclude the possibility that untreated mice succumbed from progressive *Mtb* infection, the observed gross pathological and histological characteristics in these mice were not compatible with TB-related mortality.

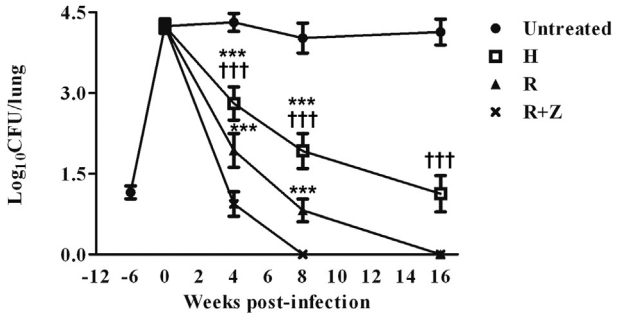

Figure 1 Validation of a paucibacillary model in C3HeB/FeJ mice. Six weeks after BCG immunization, mice were infected with *Mtb*, and 6 weeks later (week 0), treatment was initiated. Results are expressed as means ± SD of five mice per group. Colony-forming units (on TCH-containing plates) of *Mtb* in lungs. ***$P < 0.001$, R + Z versus R/H; †††$P < 0.001$, R versus H.

[^{18}F]FDG-PET activity is a marker of metabolic activity or inflammation and has been extensively used to evaluate TB lesions.[24] Diffuse [^{18}F]FDG-PET activity was noted in the lung fields of rBCG30-immunized/*Mtb*-challenged mice at the time of initiation of TNF neutralization. Mice were imaged 4 weeks later, revealing well-defined foci of increased [^{18}F]FDG uptake colocalizing with TB lesions in lung fields of control mice, and significantly higher PET activity in lungs of mice receiving anti-TNF antibody ($P = 0.004$) (Figure 2, D and E), indicating increasing inflammation with disease progression. In fact, the FDG-PET activity is highly localized to TB lesions in the untreated mice compared with more diffuse and peripheral activities in the TNF-neutralization group.

Mouse lung and spleen bacillary loads increased dramatically after 4 weeks of TNF neutralization (Figure 2, F and G), respectively. Normalized mean lung and spleen weights were significantly higher in TNF-neutralized mice relative to those of control mice ($P < 0.001$) (Figure 2, H and I), respectively. Numerous large nodules were present on the lung surface in the TNF-neutralization group (Figure 2J). Small, scattered granulomas with central caseous necrosis containing few extracellular AFB were observed at the onset of anti-TNF treatment (Figure 3, B–E). The lungs harbored zones of chronic inflammation, mainly comprising lymphocytes and macrophages, accompanied by infiltrates of granulocytes within alveolar spaces. Epithelioid macrophages and multinucleated giant cells were observed, as previously described in this mouse strain.[14] After 4 weeks of anti-TNF treatment, lung granulomas became disorganized, and consolidating lesions consistent with acute bronchopneumonia were present, which contained massive numbers of extracellular AFB within expanded foci of acute necrosis (Figure 3, F–I). There was a statistically significant ($P = 0.0002$) increase in percentage lung surface area inflammation in anti–TNF-treated mice compared with control animals (Figure 3J).

Reduced Hypoxia in Lung Lesions of Anti–TNF-Treated Mice

[^{64}Cu]ATSM is a PET imaging tracer used to detect hypoxia noninvasively. Although Cu-ATSM is cleared rapidly by euoxic cells, it is retained in oxygen-deprived, live cells and has been used to evaluate TB lesions in animal models.[11] Significantly higher [^{64}Cu]ATSM uptake was observed in untreated infected control lungs compared with those of

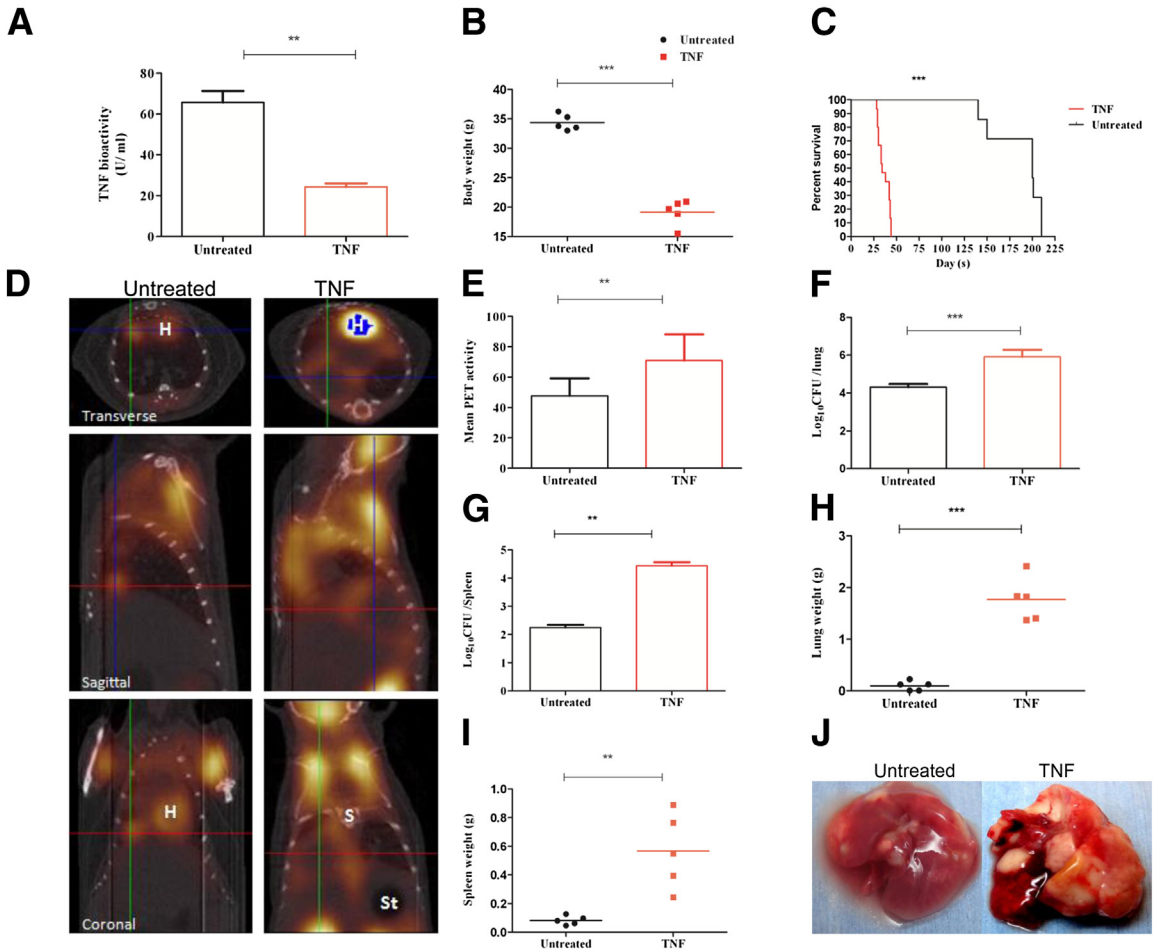

Figure 2 Reactivation of TB infection by TNF neutralization. **A:** Determination of effectiveness of TNF neutralization by WEHI bioassay. Data are normalized to the total protein concentration of lung homogenates from mice receiving anti-TNF antibodies for 4 weeks (TNF) or those receiving no treatment (untreated) and represent means ± SD for five mice. TB reactivation results in changes in total body weights (**B**) and survival proportions (**C**). Data are shown for day 0 (day of treatment initiation, which is 12 weeks after rBCG30 immunization and 6 weeks after aerosol challenge with $H_{37}Rv$) until experimental death (210 days). The *x* axis values represent days after infection. Median survival of TNF neutralization group, 34 days; untreated, 200 days. **D:** PET images of immunized C3HeB/FeJ mice challenged with $H_{37}Rv$ after TNF neutralization. [^{18}F]FDG-PET activity correlates with TB-induced lung inflammation with [^{18}F]FDG localizing to TB granulomas. Cross hair is centered over the TB lesions. **E:** [^{18}F]FDG-PET activity correlates with bacterial burden in C3HeB/FeJ mice. Mean lung PET activities for the mice treated with the MP6X22 were significantly higher than those for untreated mice. Data are means ± SD ($n = 4$ for each group). **F:** Lung bacterial burden. **G:** Colony-forming units (on TCH-containing plates) of *Mtb* in spleen. Results are expressed as means ± SD of five mice per group. Lung weights (**H**), spleen weights (**I**), and gross lung pathological characteristics of control mice (untreated) and TNF-neutralized mice (**J**). The images shown were chosen on the basis of median lung weights. $^{**}P < 0.01$, $^{***}P < 0.001$ versus untreated control. H, heart; S, sternum; St, stomach air bubble; TNF, anti-TNF monoclonal antibody.

TNF-neutralized mice 40 to 60 minutes after tracer injection ($P > 0.0001$) (Figure 4A and Supplemental Figure S1).

Pimonidazole staining was clearly noted around the periphery of the necrotic granulomas in the untreated group, whereas the analogous tissues of anti−TNF-treated mice showed markedly reduced staining (Figure 4B).

Changes in the Lung Transcriptome after TNF Neutralization

A total of 1065 genes were differentially regulated (579 were up-regulated and 486 were down- regulated) after 4 weeks of TNF neutralization (Figure 5A). Genes previously reported to be associated with human TB are functionally tabulated in Supplemental Table S1. Notably, after reactivation of infection, mouse lungs showed significant up-regulation of the following genes: the toll-like receptor genes *Tlr4*, *Tlr13*, and *Cd14*; the TNF family−like genes *Tnfaip2*, *Tnfaip3*, *Tnfrsf1a*, *Tnfrsf11*, *Tnfsf12a*, and *Tnfrsf22*; the type II arginase genes *Arg1* and *Arg2*; the transforming growth factor (TGF)-β family genes *Tgfb1*, *Ltbp4*, and *Ltb4r1*; and BclIII and *Casp4*, whose products protect T cells from cell death by apoptosis.[29,30] The matrix metalloproteinase genes *Mmp3*, *Mmp9*, *Mmp10*, *Mmp12*, *Mmp13*, *Mmp23*, and *Mmp25* were also significantly overexpressed in the lungs of TNF-neutralized mice. Genes encoding the small calcium-binding proteins S100a8, S100a9, and S100a14, which induce neutrophil chemotaxis and are expressed in TB patients,[31,32] were also up-regulated in mouse lungs after TNF neutralization. Similarly, the immunoresponsive gene1

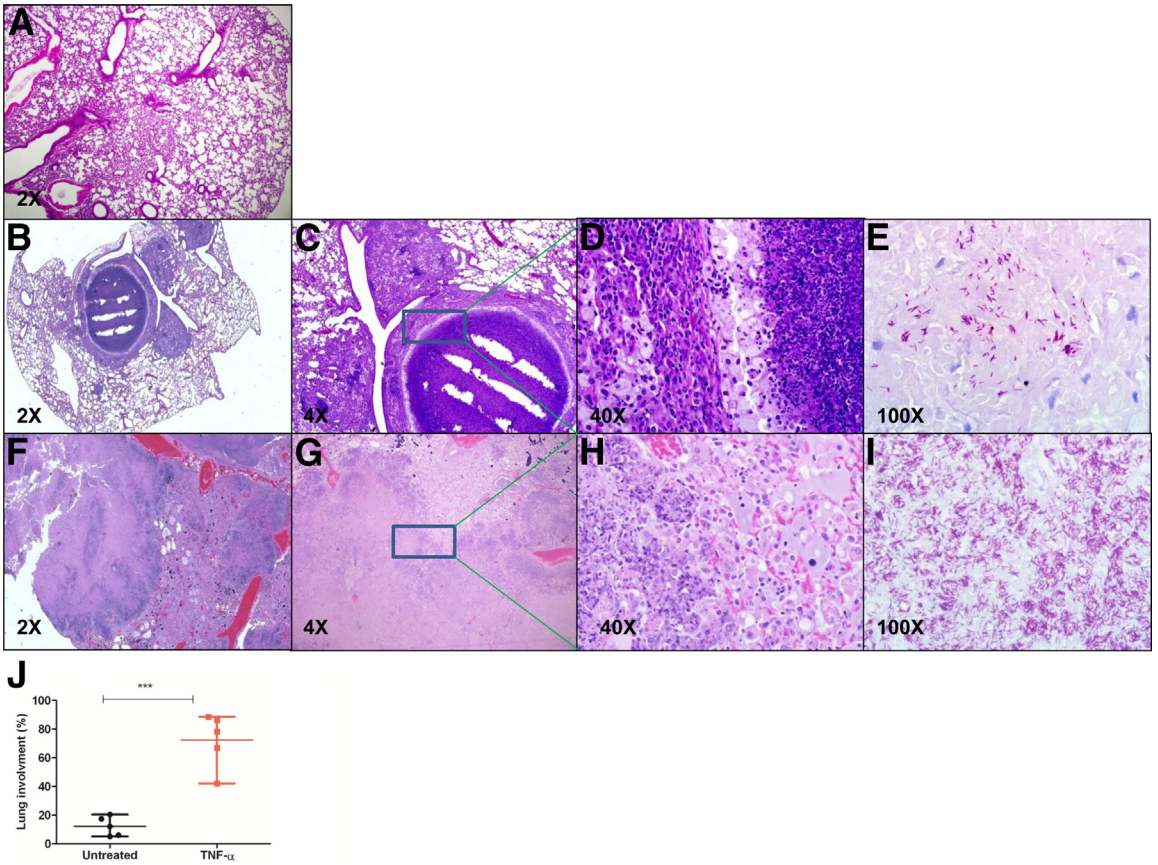

Figure 3 Histological characteristics of the lungs of mice during latent infection and reactivation. Mouse lung histopathological characteristics after anti-TNF treatment. **A:** Six weeks after immunization with rBCG30 via aerosol. **B**–**E:** Six weeks after aerosol challenge with *Mtb*. **F**–**I:** Four weeks after anti-TNF treatment. H&E staining (**A**–**D** and **F**–**H**) and acid-fast staining (**E** and **I**) were performed on lung tissues. Images shown are representative of sections obtained from five animals per group. **J:** Morphometric analysis confirmed these findings and demonstrated increased lung involvement in mice treated with anti-TNF antibodies versus untreated controls. Results are represented as percentage of lung surface area involved, calculated using image viewer software (three fields of view, obtained from five animals per group). $***P < 0.001$ versus untreated control.

(*Irg1*)[33,34] was induced. The interleukin genes *Il1a*, *Il1b*, *IL6*, and *Il11* were induced in lungs of reactivated mice, whereas the interleukin receptor genes *Il11*, *Il1r2*, *Il1rn*, *Il4i1*, and *Il8rb* were induced, and *Il11ra1* and *Il8ra* were repressed (Figure 5B).[35] Expression of several CC chemokines, such as *Ccl2* (monocyte chemoattractant protein-1), *Ccl3* (macrophage inflammatory protein-1α), *Ccl4*, *Ccl6*, *Ccl7*, and *Ccl9*, and CXC chemokines, such as *Cxcl1*, *Cxcl2*, *Cxcl4*, *Cxcl13*, *Cxcl17,* and *Cxcl19*,[36,37] were also induced in the lungs of TNF-neutralized mice (Figure 5B).

The Effect of TNF Neutralization on Several Key Immune Pathways

Major pathways that were altered after TNF neutralization included the following: regulation of cytokine production in

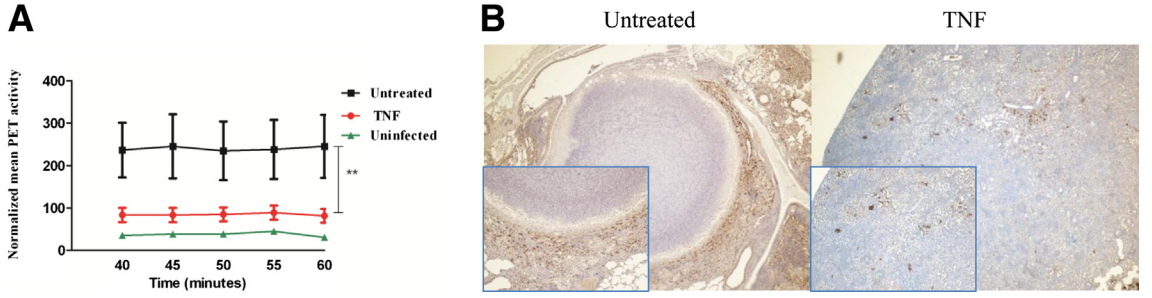

Figure 4 The *Mtb* infection and lung tissue hypoxia. PET imaging demonstrates accumulation of hypoxia probe [^{64}Cu]ATSM in tuberculosis lesions of C3HeB/FeJ mice (**A**) and its validation by pimonidazole IHC analysis (**B**). The mean [^{64}Cu]ATSM PET lung activity normalized to the thigh muscles from dynamic acquisitions is shown for rBCG30-immunized/*Mtb*-infected mice with and without anti-TNF treatment. Pimonidazole staining is observed around the periphery of the necrotic granulomas in the untreated group but is greatly reduced in the TNF-neutralization group. Data are presented as means ± SD. $**P < 0.01$ versus untreated control. Original magnification: ×4 (**B**); ×10 (**B**, **insets**).

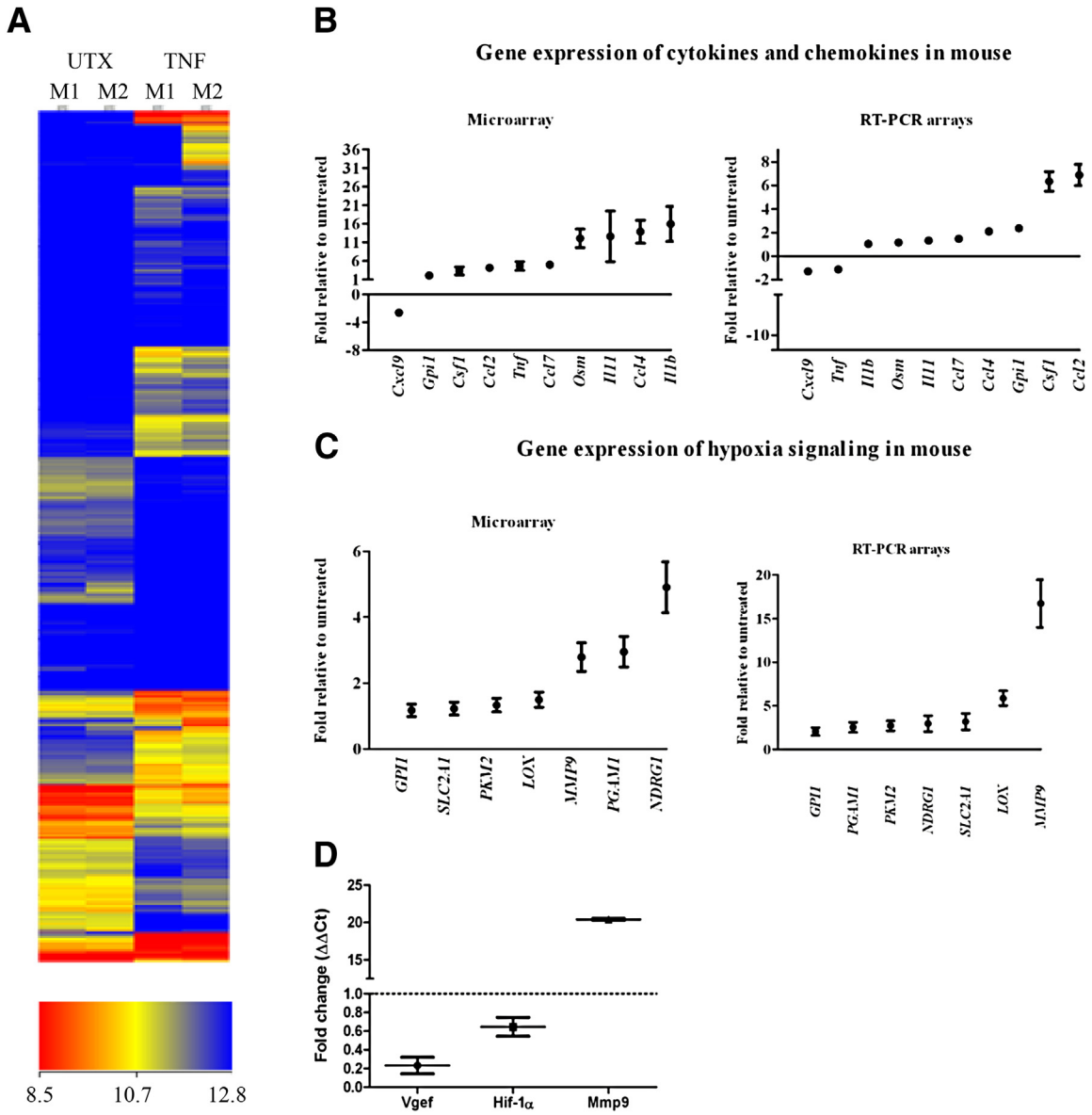

Figure 5 Cytokine gene expression signature of mice with reactivation TB. **A:** Heat map of microarray gene expression data comparing mice receiving anti-TNF antibodies for 4 weeks (TNF) with mice receiving no treatment (UTX). Values represent genes with significant change in expression ($P < 0.05$, fold change >2, $n = 1065$). Expression values are also shown for RT-PCR experiments. RT-PCR arrays specific for the mouse chemokines and cytokines (**B**) and mouse hypoxia signaling (**C**) pathway were used to confirm microarray results. The figure shows the average of two biological replicates. **D:** Gene expression profiling of granulomatous lung tissues using laser capture microdissection by RT-PCR. The values represent gene expression levels in the TNF-neutralized group relative to the untreated control group (dotted line) (means ± SD). Data in each group were normalized to a housekeeping gene before calculation of fold change. M1, mouse 1; M2, mouse 2.

macrophages and T-helper cells by IL-17A and IL-17F, histamine biosynthesis, airway pathological characteristics of chronic obstructive pulmonary disease, and superoxide radical degradation (Supplemental Figure S2). By using RT-PCR, we confirmed changes in expression of a subset of cytokine and chemokine genes, as well as those related to hypoxic signaling (Figure 5, B and C).

Hypoxia induces gene expression and secretion of many inflammatory mediators via binding of hypoxia-inducible factor 1α. Extensive lung destruction is a hallmark of pulmonary TB and is caused by breakdown of extracellular matrix by host MMPs. Consistent with the results of noninvasive [^{64}Cu]ATSM PET imaging and pimonidazole IHC analysis, lung tissues of TNF-neutralized mice showed lower expression of hypoxia-inducible genes than untreated control groups. Conversely, the MMPs were more highly expressed in the former group by microarray analysis. LCM was performed on lung tissues to determine whether our findings were granuloma specific. We observed reduced expression of *Hif-lα* and *Vegf*, and up-regulation of *Mmp9* in granulomas from TNF-neutralized mice, relative to those of control animals, consistent with reduced hypoxia and increased disruption of granuloma structure in the former group (Figure 5D).

Altered Cytokine Profiles in Whole Lungs and Sera after TNF Neutralization

By using multiplex enzyme-linked immunosorbent assays, we analyzed 23 different cytokines in the sera of untreated and TNF-neutralized mice. We found significantly increased serum levels of granulocyte colony-stimulating factor, interferon (IFN) γ, IL-1β, IL-1 receptor antagonist protein, IL-6, IL-10, IL-12 (P70), IL-13, CXCL1, and chemokine ligand (CCL) 2 in the sera of animals after TNF neutralization. Although the median absolute levels of individual cytokines were different among whole lungs and sera, there was considerable overlap in cytokine profiles between these two sources. Thus, IFN-γ, IL-1β, IL-6, IL-10, CXCL1, CCL2, and CCL3[38–40] were significantly ($P < 0.05$) more abundant in lungs and sera of TNF-neutralized mice compared with corresponding samples derived from immunized/infected control mice (Table 2).

Discussion

In the current study, we describe a novel animal model, which shares several key features of human LTBI. Specifically, this model establishes a paucibacillary infection, allowing the infected animals to survive free of symptoms for a prolonged period of time. Unlike standard mice, the C3HeB/FeJ mice used in this study develop necrotic lung granulomas, which are believed to harbor latent bacilli in humans.[7] The advantage of this model is that a clinically latent infection and human-like histopathological characteristics are achieved in a relatively economical and tractable species, compared with larger animal models of LTBI, including the rabbit and nonhuman primate. Although the absolute length of treatment with the various LTBI regimens required to achieve eradication in this model appears to differ from that observed in human LTBI, this model nevertheless recapitulates the hierarchy of sterilizing activities of these standard regimens, suggesting it may be a useful tool in assessing the treatment-shortening potential of novel LTBI regimens in humans.[18] Furthermore, as in humans,[41] paucibacillary infection can be reactivated in this model after TNF neutralization, as manifested by increasing organ bacillary loads, diffuse radiographic infiltrates, exacerbated histopathological features, and markedly accelerated weight loss and mortality.

The advent of TNF antagonist therapy for the treatment of chronic inflammatory conditions led to a stark increase in TB cases. Specifically, the incidence of TB was reported to be 144 cases per 100,000 patients treated with the humanized mouse anti-TNF monoclonal antibody infliximab. Interestingly, 44% of infliximab-related TB cases occurred within 90 days of treatment initiation, suggesting that these may represent reactivation of LTBI, perhaps due to dissolution of granuloma architecture and disseminated infection.[42] In the model described herein, we found that TNF neutralization led to increased lung inflammation overall, as manifested by increased mean lung weights and total lung uptake of [^{18}F]FDG by PET imaging. Histological analysis revealed disorganization of lung granuloma architecture with diffuse consolidation and more extensive necrosis after TNF neutralization. These findings are consistent with those of Chakravarty et al,[22] who reported that TNF blockade with MP6-XT22 led to dissolution of B-cell macrophage units in granulomatous tissues and increased inflammatory cell infiltration in the lungs of chronically infected C57BL/6 mice. We found reduced lung uptake of [^{64}Cu]ATSM by PET imaging and reduced lung lesion staining by pimonidazole in the TNF neutralization group relative to controls. Because [^{64}Cu]ATSM retention and pimonidazole staining require viable cells in the context of hypoxia,[11] it is possible that these findings simply reflect more extensive tissue necrosis in the lungs of TNF-neutralized mice. However, we observed reduced

Table 2 Concentrations of Cytokines and Chemokines in Whole Lung Homogenates and Serum, as Measured by a 23-Plex Assay

Lung homogenates				Serum		
Marker	Untreated ($n = 5$)	TNF ($n = 5$)	P value	Untreated ($n = 5$)	TNF-α ($n = 5$)	P value
GCSF	8.7	162.14 (93.83–2061.59)	0.1546	9.62 (8.7–13.72)	4338.48 (4095–4316)	2.04×10^{-10}
IFNγ	4.2	22.89 (8.29–22.89)	0.00845	4.2	16.67 (16.07–19.52)	4.24×10^{-8}
IL-1β	106.72 (89.67–127.86)	1446.58 (933.93–1495.05)	2.60×10^{-6}	79.22 (10.11–95.16)	165.08 (155.3–184.77)	0.0003
IL-1RA	13.08 (11.78–18.58)	36.09 (22.42–516.85)	0.185	3.3	515.75 (467.42–592.45)	1.14×10^{-8}
IL-6	2.1	44.94 (31.43–71.66)	0.00015	1.8	153.48 (135.87–180.55)	3.96×10^{-8}
IL-10	4.79 (4–5)	13.54 (31.54–1006.71)	0.02	21.55 (13.37–36.92)	7825.36 (7555–8050)	5.74×10^{-13}
IL-12 (P70)	9.46 (4–5)	11.22 (4.8–1734.13)	0.30298	20.1 (20.1–36.73)	11,818.83 (10,462–13,502)	1.79×10^{-8}
IL-13	40.49 (33.25–47.23)	39.76 (22.27–98.96)	0.60523	62.58 (45.7–102.06)	348.68 (315.62–404.92)	4.38×10^{-7}
KC	7.06 (6–14.35)	216.24 (153.26–489.41)	0.00234	8.41 (6.2–13.51)	205.55 (189.38–226.06)	5.20×10^{-9}
MCP-1	14.76 (12.47–15.87)	350.94 (188.88–2145.5)	0.007	20.56 (9.76–26.65)	77 (69.58–83.07)	2.08×10^{-7}
MCP-1A	6 (6–7.93)	62.71 (36.62–6366)	0.009	5.7	47.28 (45.45–53.21)	3.53×10^{-9}
TNF	27.61 (24.01–30.77)	26.05 (14.34–46.88)	0.94017	99.79 (78.59–150.66)	96.6 (93.4–111.57)	0.56188

Results are expressed as median (range). Representative qualitative levels of cytokine protein expression in whole lung homogenates and plasma from mice receiving anti-TNF antibodies for 4 weeks (TNF) or without treatment (untreated). $P < 0.05$ compared with corresponding control.

GCSF, granulocyte colony-stimulating factor; IL-1RA, IL-1 receptor antagonist protein; KC, CXCL1/KC.

pimonidazole staining even in highly cellular areas of the consolidated lung lesions in the TNF neutralization group. In addition, LCM revealed reduced expression of the hypoxia-responsive genes *Vegf* and *Hif-lα*. Expression of several matrix metalloproteinase genes, including *Mmp9*, was increased in the lungs of TNF-neutralized mice, which may account for breakdown of granuloma structure in this group. Hypoxia reduces the output of MMP-9 in monocytes by inhibiting its secretion and increasing membranal association,[43] further corroborating the hypothesis that tissue oxygen levels were higher in the lesions of TNF-neutralized animals relative to those of controls. Although our study does not allow us to unequivocally assign cause and effect, we hypothesize that TNF neutralization disrupts granuloma organization through increased expression of matrix metalloproteinases, thus increasing oxygen permeability into the lesions, which, in turn, permits bacillary regrowth.

We observed increased expression of primarily proinflammatory cytokines and chemokines in the lungs of mice after administration of MP6-XT22, likely accounting for the greater inflammation observed in these lungs by imaging and histological analysis. However, these proinflammatory responses were largely ineffective in controlling bacillary regrowth in the lungs of anti−TNF-treated mice. Similarly, Chakravarty et al[22] also reported increased expression of IFNγ, IL-10, IL-12p40, CCL2, CCL3, and CCL4 in lung lesions of chronically infected mice treated with MP6-XT22. Therefore, in addition to maintaining the structure of TB granulomas, TNF may exert an anti-inflammatory effect through modulation of the expression of proinflammatory mediators. Although our cytokine analysis by gene expression and immunoassays used whole lung homogenates rather than individual lesions, we believe that the findings are qualitatively valid, because inclusion of normal lung in each group might be expected to have the effect of dampening the total signal detected in the experimental group, but not of altering the types of cytokines expressed.

Interestingly, the serum cytokine profile we identified in TNF-neutralized mice correlates well with that observed in the corresponding lung samples. Several studies have compared serum cytokine levels in patients with active TB with those with LTBI or healthy controls. Specifically, relative to healthy controls, significantly elevated levels of IL-10, IL-12p40, TNF, and IFN-γ are seen in the sera of patients with active pulmonary TB.[38,44,45] According to a recent study, significantly increased levels of CCL2 [monocyte chemoattractant protein (MCP-1)] were detected in whole blood samples from patients with active TB compared with the LTBI group, and the combination of elevated MCP-1 and IL-15 accurately identified 83% of active infections.[46] Further corroborating our findings, previous studies have shown significantly increased levels of IL-6 in subjects with active TB compared with those with LTBI.[47] Whether these cytokine profiles in any way reflect the underlying immune pathophysiological characteristics responsible for reactivation of LTBI or whether they are merely by-products of resumed *Mtb* replication remains to be determined. In addition, their potential use as clinical biomarkers to detect subclinical active TB cases or identify persons with LTBI at increased risk for reactivation requires further study. In particular, the specificity and positive predictive value of this cytokine panel require evaluation in patients with clinical presentations mimicking TB.[48] Taken together, our data largely concur with previously published studies, further strengthening the validity of the model.

One of the limitations of our model is that paucibacillary infection is achieved after recombinant BCG vaccination, whereas such vaccination is clearly not required to control bacillary replication and establish LTBI in humans. On the other hand, we believe that our model better emulates the human condition than the Cornell model[49] in that it is dependent on immunological control of infection rather than antibiotic treatment. Moreover, the latter model is technically demanding, and the proportion of mice relapsing is variable and highly dependent on the experimental conditions, requiring many mice for adequate statistical power.[50] However, further studies will be required to validate our model and determine its utility in predicting the efficacy and safety of novel regimens for the treatment of LTBI. Eradication of infection after anti-tuberculous treatment could be confirmed by TNF neutralization, which appears to be sufficient for reactivating infection in this model.

In conclusion, we have developed a novel paucibacillary model, which may be useful in identifying the following: i) novel regimens to shorten the duration of treatment of LTBI, ii) novel biomarkers specific to the latent stage of infection and to reactivation disease, and iii) novel attenuated vaccine candidates with an inability to reactivate, which would be particularly important in the setting of HIV/AIDS.

Supplemental Data

Supplemental material for this article can be found at *http://dx.doi.org/10.1016/j.ajpath.2014.03.008*.

References

1. Manabe YC, Bishai WR: Latent Mycobacterium tuberculosis-persistence, patience, and winning by waiting. Nat Med 2000, 6: 1327−1329
2. Nuermberger EL, Yoshimatsu T, Tyagi S, Bishai WR, Grosset JH: Paucibacillary tuberculosis in mice after prior aerosol immunization with Mycobacterium bovis BCG. Infect Immun 2004, 72:1065−1071
3. Zhang T, Li SY, Williams KN, Andries K, Nuermberger EL: Short-course chemotherapy with TMC207 and rifapentine in a murine model of latent tuberculosis infection. Am J Respir Crit Care Med 2011, 184:732−737
4. Diedrich CR, Flynn JL: HIV-1/mycobacterium tuberculosis coinfection immunology: how does HIV-1 exacerbate tuberculosis? Infect Immun 2011, 79:1407−1417
5. Flynn J, Chan J: Animal models of tuberculosis. Edited by Rom W, Garay S. Tuberculosis. ed 2. Philadelphia, Lippincott Williams & Wilkins, 2004, pp 237−250

6. McMurray DN: Disease model: pulmonary tuberculosis. Trends Mol Med 2001, 7:135–137
7. Opie EL, Aronson JD: Tubercle bacilli in latent tuberculous lesions and in lung tissue without tuberculous lesions. Arch Pathol Lab Med 1927, 4:1–21
8. Lin PL, Flynn JL: Understanding latent tuberculosis: a moving target. J Immunol 2010, 185:15–22
9. Subbian S, O'Brien P, Kushner NL, Yang G, Tsenova L, Peixoto B, Bandyopadhyay N, Bader JS, Karakousis PC, Fallows D, Kaplan G: Molecular immunologic correlates of spontaneous latency in a rabbit model of pulmonary tuberculosis. Cell Commun Signal 2013, 11:16
10. Pan H, Yan BS, Rojas M, Shebzukhov YV, Zhou H, Kobzik L, Higgins DE, Daly MJ, Bloom BR, Kramnik I: Ipr1 gene mediates innate immunity to tuberculosis. Nature 2005, 434:767–772
11. Harper J, Skerry C, Davis SL, Tasneen R, Weir M, Kramnik I, Bishai WR, Pomper MG, Nuermberger EL, Jain SK: Mouse model of necrotic tuberculosis granulomas develops hypoxic lesions. J Infect Dis 2012, 205:595–602
12. Via LE, Lin PL, Ray SM, Carrillo J, Allen SS, Eum SY, Taylor K, Klein E, Manjunatha U, Gonzales J, Lee EG, Park SK, Raleigh JA, Cho SN, McMurray DN, Flynn JL, Barry CE 3rd: Tuberculous granulomas are hypoxic in guinea pigs, rabbits, and nonhuman primates. Infect Immun 2008, 76:2333–2340
13. Vilaplana C, Marzo E, Tapia G, Diaz J, Garcia V, Cardona PJ: Ibuprofen therapy resulted in significantly decreased tissue bacillary loads and increased survival in a new murine experimental model of active tuberculosis. J Infect Dis 2013, 208:199–202
14. Driver ER, Ryan GJ, Hoff DR, Irwin SM, Basaraba RJ, Kramnik I, Lenaerts AJ: Evaluation of a mouse model of necrotic granuloma formation using C3HeB/FeJ mice for testing of drugs against Mycobacterium tuberculosis. Antimicrob Agents Chemother 2012, 56:3181–3195
15. Rosenthal IM, Tasneen R, Peloquin CA, Zhang M, Almeida D, Mdluli KE, Karakousis PC, Grosset JH, Nuermberger EL: Dose-ranging comparison of rifampin and rifapentine in two pathologically distinct murine models of tuberculosis. Antimicrob Agents Chemother 2012, 56:4331–4340
16. Skerry C, Harper J, Klunk M, Bishai WR, Jain SK: Adjunctive TNF inhibition with standard treatment enhances bacterial clearance in a murine model of necrotic TB granulomas. PLoS One 2012, 7:e39680
17. Horwitz MA, Harth G: A new vaccine against tuberculosis affords greater survival after challenge than the current vaccine in the guinea pig model of pulmonary tuberculosis. Infect Immun 2003, 71:1672–1679
18. Horsburgh CR Jr, Rubin EJ: Clinical practice: latent tuberculosis infection in the United States. N Engl J Med 2011, 364:1441–1448
19. Plessner HL, Lin PL, Kohno T, Louie JS, Kirschner D, Chan J, Flynn JL: Neutralization of tumor necrosis factor (TNF) by antibody but not TNF receptor fusion molecule exacerbates chronic murine tuberculosis. J Infect Dis 2007, 195:1643–1650
20. Ahmad Z, Klinkenberg LG, Pinn ML, Fraig MM, Peloquin CA, Bishai WR, Nuermberger EL, Grosset JH, Karakousis PC: Biphasic kill curve of isoniazid reveals the presence of drug-tolerant, not drug-resistant, Mycobacterium tuberculosis in the guinea pig. J Infect Dis 2009, 200:1136–1143
21. Zhang T, Zhang M, Rosenthal IM, Grosset JH, Nuermberger EL: Short-course therapy with daily rifapentine in a murine model of latent tuberculosis infection. Am J Respir Crit Care Med 2009, 180:1151–1157
22. Chakravarty SD, Zhu G, Tsai MC, Mohan VP, Marino S, Kirschner DE, Huang L, Flynn J, Chan J: Tumor necrosis factor blockade in chronic murine tuberculosis enhances granulomatous inflammation and disorganizes granulomas in the lungs. Infect Immun 2008, 76:916–926
23. Mohan VP, Scanga CA, Yu K, Scott HM, Tanaka KE, Tsang E, Tsai MM, Flynn JL, Chan J: Effects of tumor necrosis factor alpha on host immune response in chronic persistent tuberculosis: possible role for limiting pathology. Infect Immun 2001, 69:1847–1855
24. Davis SL, Be NA, Lamichhane G, Nimmagadda S, Pomper MG, Bishai WR, Jain SK: Bacterial thymidine kinase as a non-invasive imaging reporter for Mycobacterium tuberculosis in live animals. PLoS One 2009, 4:e6297
25. Yates MD, Collins CH: Identification of tubercle bacilli. Ann Microbiol (Paris) 1979, 130B:13–19
26. Espevik T, Nissen-Meyer J: A highly sensitive cell line, WEHI 164 clone 13, for measuring cytotoxic factor/tumor necrosis factor from human monocytes. J Immunol Methods 1986, 95:99–105
27. Klinkenberg LG, Sutherland LA, Bishai WR, Karakousis PC: Metronidazole lacks activity against Mycobacterium tuberculosis in an in vivo hypoxic granuloma model of latency. J Infect Dis 2008, 198:275–283
28. Dutta NK, Mehra S, Martinez AN, Alvarez X, Renner NA, Morici LA, Pahar B, Maclean AG, Lackner AA, Kaushal D: The stress-response factor SigH modulates the interaction between Mycobacterium tuberculosis and host phagocytes. PLoS One 2012, 7:e28958
29. Mitchell TC, Hildeman D, Kedl RM, Teague TK, Schaefer BC, White J, Zhu Y, Kappler J, Marrack P: Immunological adjuvants promote activated T cell survival via induction of Bcl-3. Nat Immunol 2001, 2:397–402
30. Nickles D, Falschlehner C, Metzig M, Boutros M: A genome-wide RNA interference screen identifies caspase 4 as a factor required for tumor necrosis factor alpha signaling. Mol Cell Biol 2012, 32:3372–3381
31. Ryckman C, Vandal K, Rouleau P, Talbot M, Tessier PA: Proinflammatory activities of S100: proteins S100A8, S100A9, and S100A8/A9 induce neutrophil chemotaxis and adhesion. J Immunol 2003, 170:3233–3242
32. Vandal K, Rouleau P, Boivin A, Ryckman C, Talbot M, Tessier PA: Blockade of S100A8 and S100A9 suppresses neutrophil migration in response to lipopolysaccharide. J Immunol 2003, 171:2602–2609
33. Shi S, Blumenthal A, Hickey CM, Gandotra S, Levy D, Ehrt S: Expression of many immunologically important genes in Mycobacterium tuberculosis-infected macrophages is independent of both TLR2 and TLR4 but dependent on IFN-alphabeta receptor and STAT1. J Immunol 2005, 175:3318–3328
34. Gonzalez-Juarrero M, Kingry LC, Ordway DJ, Henao-Tamayo M, Harton M, Basaraba RJ, Hanneman WH, Orme IM, Slayden RA: Immune response to Mycobacterium tuberculosis and identification of molecular markers of disease. Am J Respir Cell Mol Biol 2009, 40:398–409
35. Marquet J, Lasoudris F, Cousin C, Puiffe ML, Martin-Garcia N, Baud V, Chereau F, Farcet JP, Molinier-Frenkel V, Castellano F: Dichotomy between factors inducing the immunosuppressive enzyme IL-4-induced gene 1 (IL4I1) in B lymphocytes and mononuclear phagocytes. Eur J Immunol 2010, 40:2557–2568
36. Kipnis A, Basaraba RJ, Orme IM, Cooper AM: Role of chemokine ligand 2 in the protective response to early murine pulmonary tuberculosis. Immunology 2003, 109:547–551
37. Maus UA, Waelsch K, Kuziel WA, Delbeck T, Mack M, Blackwell TS, Christman JW, Schlondorff D, Seeger W, Lohmeyer J: Monocytes are potent facilitators of alveolar neutrophil emigration during lung inflammation: role of the CCL2-CCR2 axis. J Immunol 2003, 170:3273–3278
38. Deveci F, Akbulut HH, Turgut T, Muz MH: Changes in serum cytokine levels in active tuberculosis with treatment. Mediators Inflamm 2005, 2005:256–262
39. Zhang M, Lin Y, Iyer DV, Gong J, Abrams JS, Barnes PF: T-cell cytokine responses in human infection with Mycobacterium tuberculosis. Infect Immun 1995, 63:3231–3234
40. Bonecini-Almeida MG, Ho JL, Boechat N, Huard RC, Chitale S, Doo H, Geng J, Rego L, Lazzarini LC, Kritski AL, Johnson WD Jr,

McCaffrey TA, Silva JR: Down-modulation of lung immune responses by interleukin-10 and transforming growth factor beta (TGF-beta) and analysis of TGF-beta receptors I and II in active tuberculosis. Infect Immun 2004, 72:2628–2634
41. Keane J, Gershon S, Wise RP, Mirabile-Levens E, Kasznica J, Schwieterman WD, Siegel JN, Braun MM: Tuberculosis associated with infliximab, a tumor necrosis factor alpha-neutralizing agent. N Engl J Med 2001, 345:1098–1104
42. Wallis RS, Broder M, Wong J, Lee A, Hoq L: Reactivation of latent granulomatous infections by infliximab. Clin Infect Dis 2005, 41(Suppl 3):S194–S198
43. Rahat MA, Marom B, Bitterman H, Weiss-Cerem L, Kinarty A, Lahat N: Hypoxia reduces the output of matrix metalloproteinase-9 (MMP-9) in monocytes by inhibiting its secretion and elevating membranal association. J Leukoc Biol 2006, 79:706–718
44. Cavalcanti YV, Brelaz MC, Neves JK, Ferraz JC, Pereira VR: Role of TNF-alpha, IFN-gamma, and IL-10 in the development of pulmonary tuberculosis. Pulm Med 2012, 2012:745483
45. Vankayalapati R, Wizel B, Weis SE, Klucar P, Shams H, Samten B, Barnes PF: Serum cytokine concentrations do not parallel Mycobacterium tuberculosis-induced cytokine production in patients with tuberculosis. Clin Infect Dis 2003, 36:24–28
46. Frahm M, Goswami ND, Owzar K, Hecker E, Mosher A, Cadogan E, Nahid P, Ferrari G, Stout JE: Discriminating between latent and active tuberculosis with multiple biomarker responses. Tuberculosis 2011, 91:250–256
47. Jones SE, Mennel RG, Brooks B, Westrick MA, Allison MA, Paulson RS, Tilmann K, Rea B: Phase II study of mitoxantrone, leucovorin, and infusional fluorouracil for treatment of metastatic breast cancer. J Clin Oncol 1991, 9:1736–1739
48. Berry MP, Graham CM, McNab FW, Xu Z, Bloch SA, Oni T, Wilkinson KA, Banchereau R, Skinner J, Wilkinson RJ, Quinn C, Blankenship D, Dhawan R, Cush JJ, Mejias A, Ramilo O, Kon OM, Pascual V, Banchereau J, Chaussabel D, O'Garra A: An interferon-inducible neutrophil-driven blood transcriptional signature in human tuberculosis. Nature 2010, 466:973–977
49. McCune RM Jr, McDermott W, Tompsett R: The fate of Mycobacterium tuberculosis in mouse tissues as determined by the microbial enumeration technique, II: the conversion of tuberculous infection to the latent state by the administration of pyrazinamide and a companion drug. J Exp Med 1956, 104:763–802
50. Lenaerts AJ, Chapman PL, Orme IM: Statistical limitations to the Cornell model of latent tuberculosis infection for the study of relapse rates. Tuberculosis (Edinb) 2004, 84:361–364